

## Minimizing interfacial losses in inverted organic solar cells comprising Al-doped ZnO

Abay Gadisa,<sup>1</sup> Yingchi Liu,<sup>2</sup> Edward T. Samulski,<sup>1</sup> and Rene Lopez<sup>2</sup>

<sup>1</sup>Department of Chemistry, Caudill and Kenan Laboratories, University of North Carolina at Chapel Hill, Chapel Hill, North Carolina CB 3290, USA

<sup>2</sup>Department of Physics and Astronomy, University of North Carolina at Chapel Hill, Phillips Hall, Chapel Hill, North Carolina CB 3255, USA

(Received 16 April 2012; accepted 3 June 2012; published online 19 June 2012)

We demonstrated a 35% enhancement in the efficiency of inverted solar cells as a result of increased open-circuit voltage and fill factor by adsorbing an ultrathin layer of a ruthenium dye N719 on an aluminum-doped zinc oxide (ZnO-Al) electron collecting interfacial layer. The interface modification with N719 changes the charge injection levels as indicated by ultraviolet photoemission spectroscopy. The efficiency of inverted solar cells comprising a bulk heterojunction photo-active film of poly(3-hexylthiophene) and phenyl-C<sub>61</sub>-butyric acid methyl ester has increased from ~2.80% to 3.80% upon employing the dye modification of the electrode interface. © 2012 American Institute of Physics. [<http://dx.doi.org/10.1063/1.4729861>]

The performance of polymer/fullerene bulk heterojunction (BHJ) solar cells has advanced greatly both in single junction<sup>1</sup> and multilayer configurations.<sup>2</sup> In recent years, inverted cell architectures have attracted attention because they essentially offer longer lifetimes compared to the traditional BHJ architecture.<sup>3–5</sup> Lifetime is an important factor that ultimately determines the commercialization and competitiveness of organic solar cells. Moreover, optimized inverted solar cells convert light to electricity at a power conversion efficiency exceeding 7%.<sup>6</sup> Inverted solar cells often utilize thin metal-oxide interfacial layers for either collection or injection of charges. For example, titanium oxide (TiO<sub>x</sub>)<sup>7,8</sup> and zinc-oxide (ZnO)<sup>9</sup> are the most commonly used n-type oxides in organic BHJ solar cells. Similarly, high work function metal-oxides such as molybdenum oxide (MoO<sub>3</sub>)<sup>10</sup> and tungsten oxide (WO<sub>3</sub>)<sup>11</sup> are also often employed for collection/injection of holes.

ZnO is one of the most prevalent oxides in organic solar cells both as a thin interfacial layer<sup>5,12</sup> and as a cathode electrode,<sup>13</sup> because of its high conductivity and excellent optical transparency. Its conductivity can be further enhanced through doping with metals such as Al. However, inverted solar cells utilizing TiO<sub>x</sub>, ZnO, and aluminum-doped ZnO (ZnO-Al) suffer from a loss of fill factor and open-circuit-voltage ( $V_{oc}$ ).<sup>14</sup> This problem is particularly acute in hybrid solar cells comprising nano-rods, or nano-wires of n-type metal-oxides into which pure electron-donor polymers, such as poly(3-hexylthiophene) (P3HT), are infiltrated.<sup>15,16</sup> The loss of  $V_{oc}$  in hybrid solar cells was attributed to backflow of charge carriers and interfacial recombination.<sup>16</sup> Similarly, conjugated polyelectrolytes were recently used in BHJ inverted solar cells to modify interface properties.<sup>17,18</sup>

In this Letter, we demonstrate enhancement of  $V_{oc}$  and fill factor in inverted solar cells comprising an ultrathin layer of a ruthenium dye N719 interfacial layer, deposited on top of an indium-tin-oxide (ITO)/glass substrate. A BHJ of P3HT and phenyl-C<sub>61</sub>-butyric acid methyl ester (PCBM) was used as an active layer. We have observed that the photovoltaic losses emanate from unfavorable current injection

levels at the ZnO-Al/organic interface. This loss is highly reduced by adsorbing N719 onto the ZnO-Al layer, resulting in a ~1% additional performance gain (up from 2.80% to 3.80%). The interface modification has led to more than a 0.5 eV shift in the work function of the ITO/ZnO-Al electrode. The work function change occurs because the dye withdraws electrons from the ZnO-Al layer and generates an electrostatic dipole at the interface.<sup>19</sup>

Pulsed laser deposition (PLD) was used to deposit a ~50 nm thick ZnO-Al layer on top of clean glass/ITO (140 nm) substrates. Deposition of ZnO-Al layer was performed at 200 °C under a 10 mTorr O<sub>2</sub> pressure, using a ZnO:Al<sub>2</sub>O<sub>3</sub> (98/2 wt. %) target. The as-prepared ITO/ZnO-Al substrates were immersed in a 0.3 mM solution of N719 in a mixture of acetonitrile and tert-butyl alcohol (1:1 by volume) at 60 °C for 5, 15, or 30 min. The substrates coated with N719 were annealed in a glove box at 140 °C for 5 min to remove the residual solvent. A solution of P3HT:PCBM (1:0.8, by wt.) was spin-cast on the substrates from a 18 mg/ml 1,2-dichlorobenzene solution, resulting into an ~80 nm thick film. The films were thermally annealed (at 140 °C for 10 min) and transferred into an evaporation chamber where WO<sub>3</sub> (3 nm) and aluminum (100 nm) back electrodes were successively thermally deposited under a shadow mask at a base pressure of  $1 \times 10^{-6}$  mbar. Current-voltage characteristics, both in the dark and under a simulated A.M. 1.5 (1000 W/m<sup>2</sup>) solar illumination (Newport), were measured using a Keithley 2400 source meter. The external quantum efficiency spectra were recorded with a lock-in amplifier under a chopped monochromatic light illumination. Device processing and photo-voltaic measurements were done in a nitrogen filled glove box ( $H_2O < 0.1$  ppm and  $O_2 < 0.1$  ppm). Optical transmission measurements were taken using a normal incidence reflection/transmission upright microscope with a conventional 4× microscope objective. Reflected light was collected via an optical fiber and analyzed with a monochromator equipped with a cooled CCD array. UPS spectra were obtained on a Kratos Axis Ultra DLD system equipped with a 21.2 eV He (I) excitation source. A pass energy of

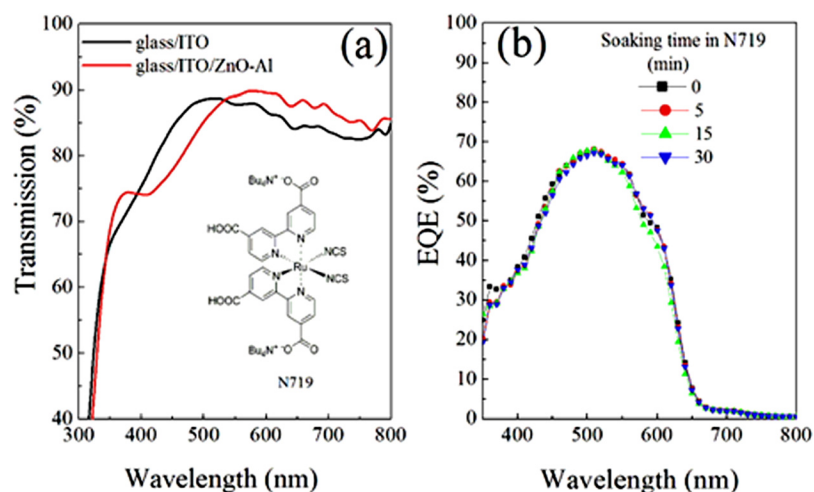


FIG. 1. (a) The optical transmittance of glass/ITO and glass/ITO/ZnO-Al substrates, and (b) the EQE of the inverted solar cells. The insert in (a) is the chemical structure of N719.

5 eV was used for all UPS analysis, and a 5 V bias was applied to the sample.

The optical transmission of glass/ITO/ZnO-Al substrates exceeded 85% in the visible region as shown in Fig. 1(a), without any significant difference from the standard glass/ITO substrates. Figure 1(b) shows the external quantum efficiency (EQE) of solar cells with or without (reference) N719. The fact that the EQE matches for all devices implies that the interfacial modification does not have a significant role on extraction of photo-current. Additionally, the matching of the EQE indicates that the N719 dye has a negligible contribution to the photocurrent. We therefore assume that the dye makes an ultrathin layer approximately equivalent to a monolayer. The photo-voltaic characteristics of the cells are depicted in Fig. 2, and the parameters extracted from this figure are displayed in Table I. Efficiencies exceeding 3.8% have been realized in the best devices. A close observation reveals that the  $V_{oc}$  and fill factor of the reference cell deviates from what is commonly achieved in conventional BHJ devices with P3HT:PCBM active layers where near 4% efficiencies are common with larger  $V_{oc}$  and fill factors.<sup>20</sup> The  $V_{oc}$  of BHJ solar cells is primarily determined by the energy of the charge transfer states formed at the polymer/fullerene interface.<sup>21</sup> The latter holds true only if electrodes are ohmic and interfacial effects originating from dipoles,<sup>19,22</sup> dark current recombination,<sup>23</sup> and interface composition<sup>24</sup> are mini-

mized. This implies that the ZnO-Al/P3HT:PCBM interface is clearly non-ohmic.

The observed photo-voltaic losses of the reference cell were reversed when a thin layer of a ruthenium dye N719 was adsorbed onto the ZnO-Al substrate (See Table I). Devices with N719 appear to have attained an optimum  $V_{oc}$  for this BHJ blend. This in turn, implies that the loss in  $V_{oc}$  originates from the quality of the ZnO-Al/organic interface. Interfacial trap-assisted recombination is a well-known loss mechanism in photo-voltaic devices.<sup>25</sup> Trap-mediated recombination is usually evident in light intensity dependent photo-voltaic measurements. To investigate this possibility, we notice that the  $V_{oc}$  of a BHJ organic solar cell, in particular, can be expressed in terms of carrier generation and recombination processes as<sup>21,26,27</sup>

$$V_{oc} = \frac{nKT}{q} \ln(J_{ph}/J_0 + 1), \quad (1)$$

where  $J_{ph}$  is the photo-generated current (the difference of the current measured under illumination and under dark conditions).  $J_0$ ,  $q$ ,  $n$ ,  $k$ , and  $T$  are the reverse saturation current density, elementary charge, diode ideality factor, Boltzmann constant, and absolute temperature, respectively. According to this formulation,  $V_{oc}$  is linked to both carrier generation and recombination processes through  $J_{ph}$  and  $n$ , respectively. The ideality factor,  $n$ , is related to charge recombination processes and, therefore, gives information on the effect of carrier traps. If  $n$  is close to 1, the carrier loss is dominated by bimolecular recombination while large values of  $n$  express trap-assisted recombination.<sup>26</sup> Figure 3 shows the measured  $V_{oc}$  of the reference solar cell as a function of incident white light intensity. Fitting the data in Fig. 3 with Eq. (1) results in an ideality factor of nearly 1, which identifies the dominant loss mechanism as bimolecular in nature for the device under white illumination.<sup>26</sup> This fit also indicates that the observed loss in  $V_{oc}$  in the reference inverted cell does not originate from traps.

The fact that  $V_{oc}$  is easily enhanced with N719 indicates that the losses are nevertheless originating at the ZnO-Al/organic interface. Modified electrodes also play major roles in determining solar cell parameters via energetic and barrier lowering effects.<sup>22-24</sup> To find out if this is the case for the N719 surface treatment, we have analyzed the ZnO-Al/

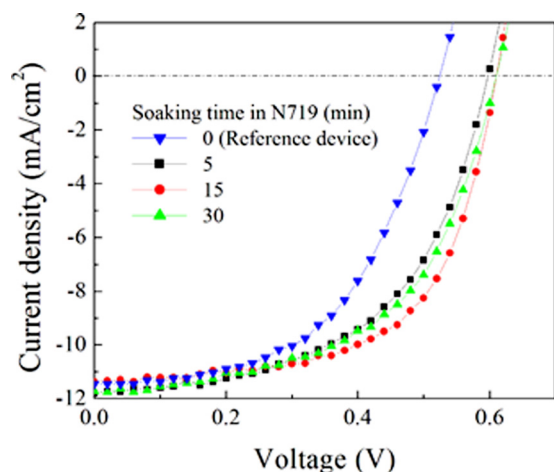


FIG. 2. The photovoltaic characteristics of the ITO/ZnO-Al/P3HT:PCBM/WO<sub>3</sub>/Al solar cells, with or without interfacial modification.

TABLE I. The photovoltaic data of the inverted solar cells as extracted from Fig. 2, series resistance, shunt resistance, and reverse saturation current. The reverse saturation current was extracted from the current-voltage characteristics measured under dark.

Soaking time in N719 (min)	$J_{sc}$ (mA/cm <sup>2</sup> )	$V_{oc}$ (V)	FF(%)	Efficiency (%)	$R_s$ ( $\Omega$ cm <sup>2</sup> )	$R_{sh}$ ( $\Omega$ cm <sup>2</sup> )	$J_0$ (mA/cm <sup>2</sup> )
0	10.22	0.56	48.81	2.79	21.03	273.77	$1.20 \times 10^{-2}$
5	10.54	0.60	56.03	3.54	13.43	550.21	$3.65 \times 10^{-4}$
15	10.46	0.61	60.00	3.83	11.01	829.51	$7.85 \times 10^{-4}$
30	10.66	0.60	53.83	3.42	14.03	506.36	$4.2 \times 10^{-4}$

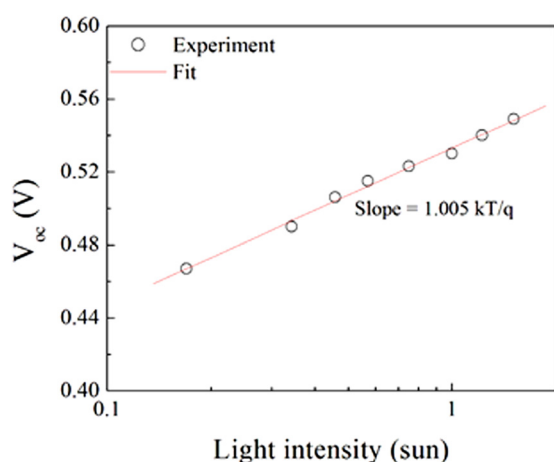


FIG. 3. Light intensity dependence of the  $V_{oc}$  of the reference cell, which comprises no dye interlayer.

organic interface using UPS. The work function of the bare ITO/ZnO-Al substrate was determined to be 3.78 eV as calculated from the UPS spectra depicted in Fig. 4. The N719 treatment resulted in a shift in the secondary edge to higher binding energy, giving rise to a work function of 4.33 eV. This kind of shift in energy has been suggested to originate from the formation of interfacial dipoles as result of N719 withdrawing electrons from ZnO-Al.<sup>19</sup> These interfacial changes determine the dark current injection level, which in turn gives rise to changes in  $V_{oc}$  in agreement with Eq. (1). The saturation current density, which was calculated from the current-voltage characteristics measured in the dark, is displayed in Table I.

On the other hand, the fill factor was also considerably enhanced in the modified devices. We attribute the increase in

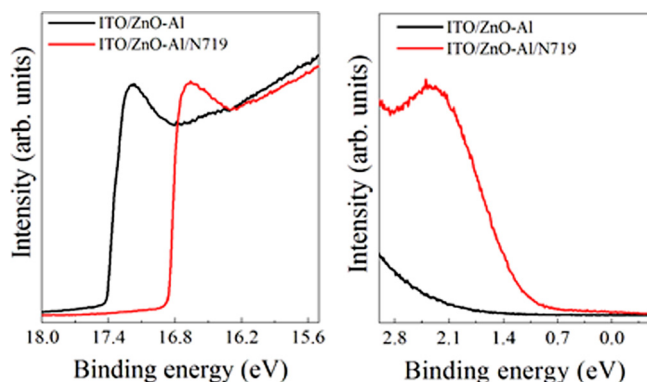


FIG. 4. The UPS measurements of ITO/ZnO-Al substrate with and without N719 interlayer. The figures show the secondary-electron cutoff of the UPS spectra from which the work function of the substrates are determined.

fill factor to the reduction of the series resistance, lowering of the injected dark current (due to the increased work function) on using N719. It is also noted that the shunt resistance has been considerably changed in the modified devices (Table I). For a device under illumination, large inflow of dark current distorts the shape of the current-voltage characteristics, thereby leading to a change in fill factor as well as  $V_{oc}$ . By and large, our results have clearly demonstrated the crucial role that interfaces play in inverted organic solar cells with P3HT:PCBM BHJ photo-active layers. The performance of the investigated devices can be further improved upon optimizing the conductivity of the ZnO-Al layer and reducing the series resistance. The latter work is currently under investigation and beyond the scope of the current report.

In conclusion, we have demonstrated that inverted solar cells built on ITO/ZnO-Al substrates deliver efficiencies exceeding 3.8%, after interface losses are minimized through inclusion of an ultrathin layer of a ruthenium dye N719. Treating the ZnO-Al layer with the N719 dye has resulted in an increased electrode work function, a reduced series resistance and an enhanced shunt resistance, which leads to an increased  $V_{oc}$  and fill factor.

Support for this work from NSF (Solar: DMR-0934433) is gratefully acknowledged. We thank Dr. Yukihiro Hara for helpful discussions.

<sup>1</sup>Y. Liang, Z. Xu, J. Xia, S.-T. Tsai, Y. Wu, G. Li, C. Ray, and L. Yu, *Adv. Mater.* **22**, E135 (2010).

<sup>2</sup>L. Dou, J. You, J. Yang, C.-C. Chen, Y. He, S. Murase, T. Moriarty, K. Emery, G. Li and Y. Yang, *Nat. Photonics* **6**, 180 (2012).

<sup>3</sup>H.-L. Yip and A. K.-Y. Jen, *Energy Environ. Sci.* **5**, 5994 (2012).

<sup>4</sup>B. Zimmermann, U. Wurfel, and M. Niggemann, *Sol. Energy Mater. Sol. Cells* **93**, 491 (2009).

<sup>5</sup>Y. Sun, J. H. Seo, C. J. Takacs, J. Seifert, and A. J. Heeger, *Adv. Mater.* **23**, 1679 (2011).

<sup>6</sup>C. E. Small, S. Chen, J. Subbiah, C. M. Amb, S. W. Tsang, T. H. Lai, J. R. Reynolds, and F. So, *Nat. Photonics* **6**, 115 (2012).

<sup>7</sup>R. Steim, S. A. Choulis, P. Schilinsky, and C. J. Brabec, *Appl. Phys. Lett.* **92**, 093303 (2008).

<sup>8</sup>S. H. Park, A. Roy, S. Beaupré, S. Cho, N. Coates, J. S. Moon, D. Moses, M. Leclerc, K. Lee, and A. J. Heeger, *Nat. Photonics* **3**, 297 (2009).

<sup>9</sup>J. Gilot, M. M. Wienk, and R. A. J. Janssen, *Appl. Phys. Lett.* **90**, 143512 (2007).

<sup>10</sup>P. de Bruyn, D. J. D. Moet, and P. W. M. Blom, *Org. Electron.* **11**, 1419 (2010).

<sup>11</sup>C. Tao, S. Ruan, G. Xie, X. Kong, L. Shen, F. Meng, C. Liu, X. Zhang, W. Dong, and W. Chen, *Appl. Phys. Lett.* **94**, 043311 (2009).

<sup>12</sup>Z. Liang, Q. Zhang, O. Wiranwetchayan, J. Xi, Z. Yang, K. Park, C. Li, and G. Cao, *Adv. Funct. Mater.* **22**, 2194 (2012).

<sup>13</sup>A. De Sio, K. Chakanga, O. Sergeev, K. von Maydell, J. Parisi, and E. von Hauff, *Sol. Energy Mater. Sol. Cells* **98**, 52 (2012).

<sup>14</sup>J. Huang, Z. Yinb, and Q. Zheng, *Energy Environ. Sci.* **4**, 3861 (2011).

<sup>15</sup>D. C. Olson, J. Piris, R. T. Collins, S. E. Shaheen, and D. S. Ginley, *Thin Solid Films* **496**, 26 (2006).

- <sup>16</sup>Y.-Y. Lin, Y.-Y. Lee, L. Chang, J.-J. Wu, and C.-W. Chen, *Appl. Phys. Lett.* **94**, 063308 (2009).
- <sup>17</sup>J. H. Seo, A. Gutacker, Y. Sun, H. Wu, F. Huang, Y. Cao, U. Scherf, A. J. Heeger, and G. C. Bazan, *J. Am. Chem. Soc.* **133**, 8416 (2011).
- <sup>18</sup>H. Choi, J. S. Park, E. Jeong, G.-H. Kim, B. R. Lee, S. O. Kim, M. H. Song, H. Y. Woo, and J. Y. Kim, *Adv. Mater.* **23**, 2759 (2011).
- <sup>19</sup>J. E. Lyon, M. K. Rayan, M. M. Beerbom, and R. Schlaf, *J. Appl. Phys.* **104**, 073714 (2008).
- <sup>20</sup>G. Dennler, M. C. Scharber, and C. J. Brabec, *Adv. Mater.* **21**, 1323 (2009).
- <sup>21</sup>K. Vandewal, K. Tvingstedt, A. Gadisa, O Inganas, and J. V. Manca, *Nature Mater.* **8**, 904 (2009).
- <sup>22</sup>H. Kim, J. H. Seo, and S. Cho, *Appl. Phys. Lett.* **99**, 213302 (2011).
- <sup>23</sup>Y.-X. Wang, S.-R. Tseng, H.-F. Meng, K.-C. Lee, C.-H. Liu, and S.-F. Horng, *Appl. Phys. Lett.* **93**, 133501 (2008).
- <sup>24</sup>N. D. Treat, L. M. Campos, M. D. Dimitriou, B. Ma, M. L. Chabinyc, and C. J. Hawker, *Adv. Mater.* **22**, 4982 (2010).
- <sup>25</sup>W. L. Leong, S. R. Cowan, and A. J. Heeger, *Adv. Energy Mater.* **1**, 517 (2011).
- <sup>26</sup>G. A. H. Wetzelaer, M. Kuik, M. Lenes, and P. W. M. Blom, *Appl. Phys. Lett.* **99**, 153506 (2011).
- <sup>27</sup>M. D. Perez, C. Borek, S. R. Forrest, and M. E. Thompson, *J. Am. Chem. Soc.* **131**, 9281 (2009).